




Assessing wind energy potential using finite mixture distributions

Melih Burak KOCA*, Muhammet Burak KILIÇ, Yusuf ŞAHİN

Department of Business Administration, Faculty of Economics and Administrative Sciences,
Burdur Mehmet Akif Ersoy University, Burdur, Turkey

Received: 12.02.2018

Accepted/Published Online: 30.12.2018

Final Version: 15.05.2019

Abstract: Wind has become a popular renewable energy resource in the last two decades. Wind speed modeling is a crucial task for investors to estimate the energy potential of a region. The aim of this paper was to compare the popular unimodal wind speed distributions with their two-component mixture forms. Accordingly, Weibull, gamma, normal, lognormal distributions, and their two-component mixture forms; two-component mixture Weibull, two-component mixture gamma, two-component mixture normal, and two-component mixture lognormal distributions were employed to model wind speed datasets obtained from Belen Wind Power Plant and Gökçeada Meteorological Station. This paper also provides the comparison of gradient-based and gradient-free optimization algorithms for maximum likelihood (ML) estimators of the selected wind speed distributions. ML estimators of the distributions were obtained by using Newton–Raphson, Broyden–Fletcher–Goldfarb–Shanno, Nelder–Mead, and simulated annealing algorithms. Fit performances were compared based on Kolmogorov–Smirnov test, root mean square error, coefficient of determination (R^2), and power density error criteria. Results reveal that two-component mixture wind speed distributions have superiority over the unimodal wind speed distributions.

Key words: Finite mixture distributions, wind energy, wind speed modeling, optimization algorithms

1. Introduction

As demand of energy increases with the population growth, renewable energy resources have started to play an important role in meeting the energy needs. Recently, the fossil fuel reserves have gradually decreased and the interest in the clean and renewable energy resources has increased [1–4]. There are several forms of renewable energy such as hydro energy, wind energy, solar energy, geothermal energy, and biomass energy. Among these renewable energy resources, wind energy has become a growing interest in recent years. There are significant increases in the number of wind energy plants installed in Turkey and the whole world. By the end of 2016, Turkey had 6106.05 MW installed wind energy capacity [5] and the wind energy potential of Turkey was predicted as 48,000 MW¹, which is more than 11% of the global installed wind energy capacity in 2016. Global wind power had an average annual growth rate of 22.1% between 1990 and 2015 [5]. Figures 1a and 1b show the cumulative installed wind energy capacity of Turkey and the world.

The different events of solar heating on the Earth's surface cause temperature and pressure differences in different regions. These differences of pressure lead air to move to other regions with low air pressure. This

*Correspondence: mbkoca@mehmetakif.edu.tr

¹Republic of Turkey Ministry of Energy and Natural Resources. (2019). Wind [online]. Website <http://www.enerji.gov.tr/en-US/Pages/Wind> [accessed 25 January 2019]

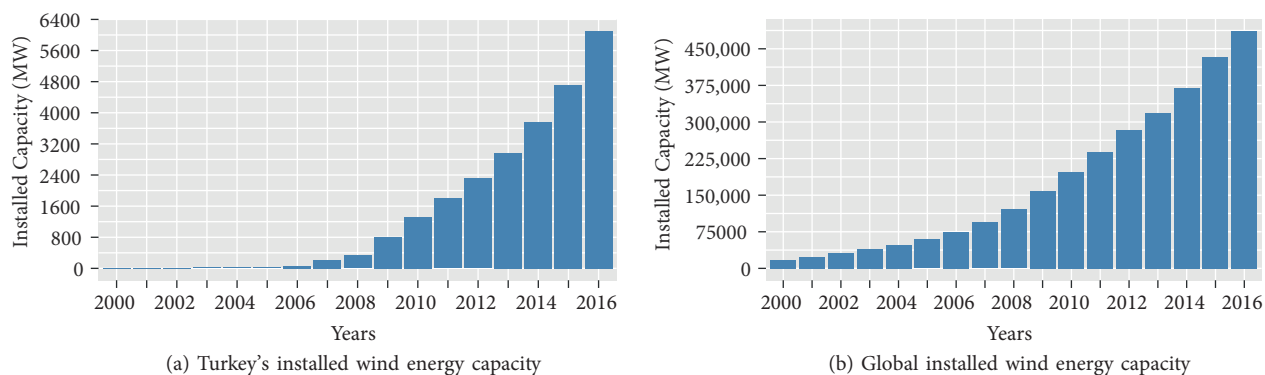


Figure 1. Cumulative installed wind energy capacity of Turkey and the world.

movement generates air currents which carry kinetic energy. Wind turbines convert the kinetic energy carried by air currents to mechanical or electrical energy [6]. Wind is a renewable, clean, and never-ending source of energy; however, the initial investment cost of turbines required to produce energy is high. Therefore, estimating the energy potential of the region is a critical prerequisite for entrepreneurs who are considering investment. It is also important for choosing the proper turbine model. Wind speed is the most important variable in the calculation of wind energy potential that is highly dependent on wind speed data [7, 8]. Wind speed modeling and estimation of wind energy potential have become the subject of many works in recent years.

Unimodal wind speed distributions are being highly used for wind speed modeling and wind power potential evaluation studies. Especially, two-parameter Weibull distribution is the most commonly used wind speed distribution due to its simplicity and flexibility in many wind energy studies. Beside Weibull distribution, other unimodal distributions such as Rayleigh, gamma, normal, and lognormal are also being used.

In the literature of unimodal wind speed distributions, Safari [6] compared Weibull, Rayleigh, lognormal, normal, and gamma distributions for modeling the wind speed data and found that Weibull, lognormal, and gamma distributions provide better fit for the data observed. Kaplan [9], Köse et al. [10], Çelik [11], Akpınar and Akpınar [12], and Gökçek et al. [13] employed Weibull and Rayleigh distributions to evaluate the wind energy potential in their studies. Hou et al. [7] showed that gamma and lognormal distributions performed better than Weibull distribution in some occasions. Akgül et al. [14] suggested that inverse Weibull distribution is a good alternative to the conventional Weibull distribution. Kantar and Usta showed that the minimum cross entropy [15] and the upper-truncated Weibull distribution [16] are better alternatives to the Weibull distribution. Sohoni et al. [8] compared Weibull, Rayleigh, gamma, lognormal, and inverse Gaussian distributions. They revealed that Weibull, Rayleigh, and gamma distributions represent the data better. Mert and Karakuş [17] employed 4-parameter Burr, 3-parameter generalized gamma, and Weibull distributions to analyze wind speed data obtained from Hatay, Turkey. Arslan et al. [18] proposed generalized Lindley and power Lindley distributions as alternative to Weibull distribution. Kantar et al. [19] employed the extended generalized Lindley distribution (EGLD) for wind speed analysis and they revealed that EGLD outperforms well-known unimodal distributions including Weibull, Rayleigh, gamma, and lognormal. Even though unimodal distributions are highly popular in wind speed modeling studies, they remain incapable of providing a good fit for the observations from the heterogeneous wind regime. Therefore, finite mixture distributions are also being employed.

In the literature of mixture wind speed distributions, Morgan et al. [20] stated that when Weibull distribution is compared with the more complex models such as two-component mixture Weibull (WW),

Kappa and Wakeby, it provides poor fit. Kollu et al. [21] described three mixture distribution functions including Weibull-extreme value distribution (GEV), Weibull-lognormal, and GEV-lognormal, they revealed that mixture distributions including GEV are superior to conventional Weibull, WW, gamma, and lognormal distributions. Akpınar and Akpınar [2] employed Weibull, WW, the maximum entropy principle (MEP) and the singly truncated from below normal Weibull mixture (TNW) distributions. Carta and Ramirez [22] compared Weibull distribution with TNW and WW distributions. Usta and Kantar [23] employed skewed generalized error distribution (SGED), and skewed t distribution (STD) in wind speed modeling. They showed that SGED and STD performed better than two- and three-parameter Weibull distributions. Chang [24] compared 6 distributions including Weibull, mixture of gamma and normal, NN, mixture of normal and Weibull, WW, and MEP. Akdağ et al. [25] and Jaramillo and Borja [26] showed the superiority of WW to conventional Weibull distribution in their studies. Shin et al. [27] utilized various homogeneous and heterogeneous mixture distributions, and they found that Weibull-extreme value type-one mixture distribution is the most appropriate distribution for the wind speed data observed in the UAE. Mazzeo et al. [28] proposed a mixture of two truncated normal distributions to model wind speed data obtained from several locations.

The main contribution of this paper is the comparison of maximum likelihood (ML) estimators of the unimodal and two-component mixture wind speed distributions by using Newton–Raphson (NR), Broyden–Fletcher–Goldfarb–Shanno (BFGS), Nelder–Mead (NM), and simulated annealing (SA) optimization algorithms for the datasets obtained from an actual wind farm and a meteorological station. Our motivation can be seen from Figures 2a–2c, where the empirical wind speed density functions are highly heterogeneous. To assess the fit performances of wind speed distribution functions, Kolmogorov–Smirnov (K-S) test, root mean square error (RMSE), coefficient of determination (R^2), and power density error (PDE) were considered as judgment criteria. Computation times were also included for a fair assessment. The rest of this paper is organized as follows: Section 2 describes the conventional unimodal and two-component mixture wind speed distributions, parameter estimation method, optimization algorithms, and model assessment criteria. A detailed information about the datasets and assessments of chosen wind speed distributions are presented in Section 3. Section 4 presents some aspects of the study. Finally, Section 5 includes the concluding remarks.

2. Materials and methods

Numerous wind speed distributions have been used in previous studies. The most common ones, Weibull, gamma, normal, and lognormal distributions, and their two-component mixture forms were considered in this paper. To find the unknown parameters of wind speed distributions, we used the ML approach which is the most common estimation technique in wind energy studies. NR, BFGS, NM, and SA algorithms were used to obtain ML estimators of the selected wind speed distributions.

2.1. Unimodal wind speed distributions

2.1.1. The Weibull distribution

One of the most frequently used distributions in wind speed modeling is the Weibull distribution. Let V be a random variable, the probability density function (*pdf*), and cumulative distribution function (*cdf*) of the Weibull distribution are respectively given by:

$$f(v; k, c) = \frac{k}{c} \left(\frac{v}{c}\right)^{k-1} \exp\left[-\left(\frac{v}{c}\right)^k\right] \quad (1)$$

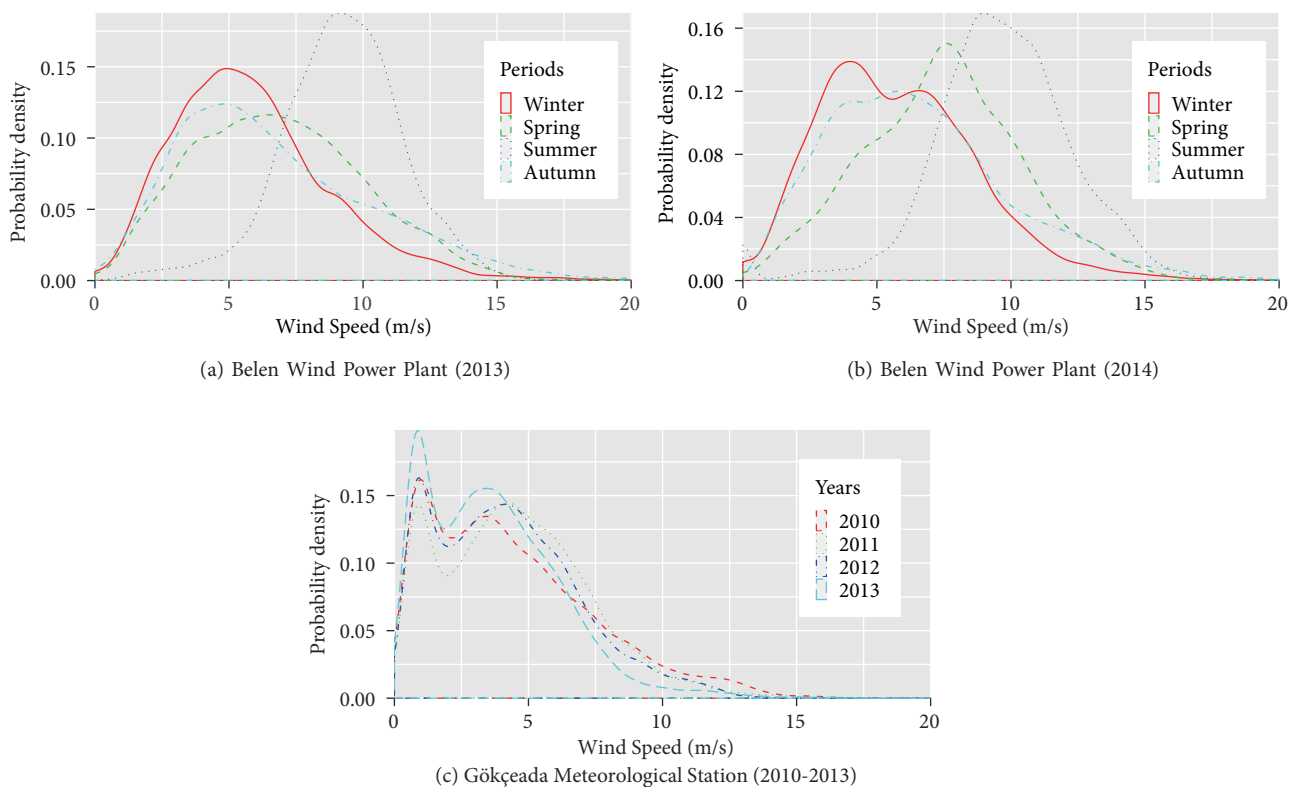


Figure 2. Empirical probability density functions.

and

$$F(v; k, c) = 1 - \exp\left[-\left(\frac{v}{c}\right)^k\right], \tag{2}$$

where v is the wind speed data, k and c are the shape and scale parameters, respectively. ML estimators for k and c can be obtained by maximizing the log-likelihood function as shown below:

$$\ln L_{Weibull} = \sum_{i=1}^n \ln\{f(v_i; k, c)\}, \tag{3}$$

where v_i denotes the wind speed observations and n is the number of observations. The ML estimators of k and c are respectively given below:

$$\hat{k} = \left[\frac{\sum_{i=1}^n v_i^{\hat{k}} \ln(v_i)}{\sum_{i=1}^n v_i^{\hat{k}}} - \frac{\sum_{i=1}^n \ln(v_i)}{n} \right]^{-1} \tag{4}$$

and

$$\hat{c} = \left[\frac{1}{n} \sum_{i=1}^n v_i^{\hat{k}} \right]^{1/\hat{k}}. \tag{5}$$

However, the ML estimator of k can be computed by iterative methods.

2.1.2. Gamma distribution

The *pdf* and *cdf* of gamma distribution are respectively given below:

$$f(v; \alpha, \beta) = \frac{v^{\alpha-1}}{\beta^\alpha \Gamma(\alpha)} \exp \left[-\frac{v}{\beta} \right] \tag{6}$$

and

$$F(v; \alpha, \beta) = \int \frac{v^{\alpha-1}}{\beta^\alpha \Gamma(\alpha)} \exp \left[-\frac{v}{\beta} \right] dv, \tag{7}$$

where α and β are the shape and scale parameters respectively, and $\Gamma(\alpha)$ is the gamma function. The log-likelihood function of gamma distribution is given below:

$$\ln L_{Gamma} = \sum_{i=1}^n \ln \{ f(v_i; \alpha, \beta) \} \tag{8}$$

2.1.3. Normal distribution

Normal distribution has two parameters: μ and σ that are called mean and variance, respectively. The *pdf* and *cdf* of normal distribution are respectively given below:

$$f(v; \mu, \sigma) = \frac{1}{\sigma \sqrt{2\pi}} \exp \left[-\frac{(v - \mu)^2}{2\sigma^2} \right] \tag{9}$$

and

$$F(v; \mu, \sigma) = \frac{1}{2} \left[1 + \operatorname{erf} \left(\frac{v - \mu}{\sigma \sqrt{2}} \right) \right]. \tag{10}$$

The log-likelihood function of normal distribution is given by:

$$\ln L_{Normal} = \sum_{i=1}^n \ln \{ f(v_i; \mu, \sigma) \}. \tag{11}$$

2.1.4. Lognormal distribution

The *pdf* and *cdf* of lognormal distribution are respectively given by:

$$f(v; \mu, \sigma) = \frac{1}{\sigma v \sqrt{2\pi}} \exp \left[-\frac{(\ln v - \mu)^2}{2\sigma^2} \right] \tag{12}$$

and

$$F(v; \mu, \sigma) = \frac{1}{2} \left[1 + \operatorname{erf} \left(\frac{\ln v - \mu}{\sigma \sqrt{2}} \right) \right], \tag{13}$$

where μ and σ are the mean and variance of the $\ln v$, respectively. The log-likelihood function of lognormal distribution is given by:

$$\ln L_{Lognormal} = \sum_{i=1}^n \ln \{ f(v_i; \mu, \sigma) \} \tag{14}$$

2.2. Mixture wind speed distributions

2.2.1. Two-component mixture Weibull distribution

The *pdf* and the *cdf* of WW are respectively given by:

$$f(v; p, k_1, c_1, k_2, c_2) = p \frac{k_1}{c_1} \left(\frac{v}{c_1}\right)^{k_1-1} \exp\left[-\left(\frac{v}{c_1}\right)^{k_1}\right] + (1-p) \frac{k_2}{c_2} \left(\frac{v}{c_2}\right)^{k_2-1} \exp\left[-\left(\frac{v}{c_2}\right)^{k_2}\right] \quad (15)$$

and

$$F(v; p, k_1, c_1, k_2, c_2) = p \left\{1 - \exp\left[-\left(\frac{v}{c_1}\right)^{k_1}\right]\right\} + (1-p) \left\{1 - \exp\left[-\left(\frac{v}{c_2}\right)^{k_2}\right]\right\}, \quad (16)$$

where k_1 and c_1 are the shape and scale parameters of the first Weibull component. Similarly, k_2 and c_2 are the shape and scale parameters of the second Weibull component. p is the mixing parameter where $0 < p < 1$. The log-likelihood function of WW is given below:

$$\ln L_{WW} = \sum_{i=1}^n \ln \{pf(v_i; k_1, c_1) + (1-p)f(v_i; k_2, c_2)\} \quad (17)$$

2.2.2. Two-component mixture gamma distribution

The *pdf* and *cdf* of GG are respectively given as follows:

$$f(v; p, \alpha_1, \beta_1, \alpha_2, \beta_2) = p \frac{v^{\alpha_1-1}}{\beta_1^{\alpha_1} \Gamma(\alpha_1)} \exp\left[-\frac{v}{\beta_1}\right] + (1-p) \frac{v^{\alpha_2-1}}{\beta_2^{\alpha_2} \Gamma(\alpha_2)} \exp\left[-\frac{v}{\beta_2}\right] \quad (18)$$

and

$$F(v; p, \alpha_1, \beta_1, \alpha_2, \beta_2) = p \int \frac{v^{\alpha_1-1}}{\beta_1^{\alpha_1} \Gamma(\alpha_1)} \exp\left[-\frac{v}{\beta_1}\right] dv + (1-p) \int \frac{v^{\alpha_2-1}}{\beta_2^{\alpha_2} \Gamma(\alpha_2)} \exp\left[-\frac{v}{\beta_2}\right] dv, \quad (19)$$

where α_1 and β_1 are the shape and scale parameters of the first gamma component, α_2 and β_2 are the shape and scale parameters of the second gamma component respectively. p is the mixing parameter where $0 < p < 1$. The log-likelihood function of GG is given below:

$$\ln L_{GG} = \sum_{i=1}^n \ln \{pf(v_i; \alpha_1, \beta_1) + (1-p)f(v_i; \alpha_2, \beta_2)\}. \quad (20)$$

2.2.3. Two-component mixture normal distribution

The *pdf* and the *cdf* of NN are respectively given by:

$$f(v; \mu_1, \sigma_1, \mu_2, \sigma_2) = p \frac{1}{\sigma_1 \sqrt{2\pi}} \exp\left[-\frac{(v - \mu_1)^2}{2\sigma_1^2}\right] + (1-p) \frac{1}{\sigma_2 \sqrt{2\pi}} \exp\left[-\frac{(v - \mu_2)^2}{2\sigma_2^2}\right] \quad (21)$$

and

$$F(v; p, \mu_1, \sigma_1, \mu_2, \sigma_2) = \frac{p}{2} \left[1 + \operatorname{erf}\left(\frac{v - \mu_1}{\sigma_1 \sqrt{2}}\right)\right] + \frac{(1-p)}{2} \left[1 + \operatorname{erf}\left(\frac{v - \mu_2}{\sigma_2 \sqrt{2}}\right)\right], \quad (22)$$

where μ_1 and σ_1 are the mean and variance of the first normal component respectively. Similarly, μ_2 and σ_2 are the mean and variance of the second normal component. p is the mixing parameter and $0 < p < 1$. The log-likelihood function of NN is given as follows:

$$\ln L_{NN} = \sum_{i=1}^n \ln \{pf(v_i; \mu_1, \sigma_1) + (1-p)f(v_i; \mu_2, \sigma_2)\} \quad (23)$$

2.2.4. Two-component mixture lognormal distribution

The *pdf* and the *cdf* of LL are respectively given as follows:

$$f(v; \mu_1, \sigma_1, \mu_2, \sigma_2) = p \frac{1}{\sigma_1 v \sqrt{2\pi}} \exp \left[\frac{-(\ln v - \mu_1)^2}{2\sigma_1^2} \right] + (1-p) \frac{1}{\sigma_2 v \sqrt{2\pi}} \exp \left[\frac{-(\ln v - \mu_2)^2}{2\sigma_2^2} \right] \quad (24)$$

and

$$F(v; p, \mu_1, \sigma_1, \mu_2, \sigma_2) = \frac{p}{2} \left[1 + \operatorname{erf} \left(\frac{\ln v - \mu_1}{\sigma_1 \sqrt{2}} \right) \right] + \frac{(1-p)}{2} \left[1 + \operatorname{erf} \left(\frac{\ln v - \mu_2}{\sigma_2 \sqrt{2}} \right) \right], \quad (25)$$

where μ_1 and σ_1 are the mean and variance of the first lognormal component, respectively. μ_2 and σ_2 are the mean and variance of the second lognormal component, p is the mixing parameter where $0 < p < 1$. The log-likelihood function of LL is given by:

$$\ln L_{LL} = \sum_{i=1}^n \ln \{ p f(v_i; \mu_1, \sigma_1) + (1-p) f(v_i; \mu_2, \sigma_2) \}. \quad (26)$$

2.3. Maximum likelihood estimation

The main idea of the ML approach is based on the maximization of the log-likelihood function given in Eqs. (3), (8), (11), (14), (17), (20), (23), and (26). ML estimations are the solutions of the first order partial derivatives of log-likelihood functions and they can be solved numerically using optimization techniques. To obtain ML estimators of the parameters, we use maxLik function which allows to select different optimization algorithms including NR, BFGS, NM, and SA in R software [29].

2.3.1. The Newton–Raphson algorithm

NR is a simple and powerful algorithm. Let x_0 be the initial value for a root of a differentiable function f , ∇ is the gradient vector and H is the Hessian matrix (a matrix obtained from second partial derivatives of f). First iteration will be

$$x_1 = x_0 - H^{-1}(x_0) \nabla(x_0) \quad (27)$$

iterations more generally

$$x_{(i+1)} = x_i - H^{-1}(x_i) \nabla(x_i), \quad (28)$$

where i is the number of iterations. Iterations will stop when $\|x_{(i+1)} - x_i\| < c$ where c is a predefined constant. NR is a fast algorithm, it converges quadratically; however, the success of the algorithm highly depends on the initial values. Another major disadvantage of NR is that it requires to compute Hessian matrix and gradient vector at each iteration.

2.3.2. The Broyden–Fletcher–Goldfarb–Shanno algorithm

BFGS [30–33] is a very powerful technique in solving unconstrained optimization problems. BFGS does not explicitly compute the Hessian but it approximates; therefore, it is a fast algorithm. BFGS updates the Hessian at each iteration by using the following formula:

$$V_{k+1} = \left[I - \frac{s_k y_k^T}{s_k^T y_k} \right] V_k \left[I - \frac{y_k s_k^T}{s_k^T y_k} \right] + \frac{s_k s_k^T}{s_k^T y_k}, \quad (29)$$

where k is the iteration number, x_k is the starting point, $V_k \approx H_k^{-1}$, s_k is the step taken from x_k and $y_k = H_k s_k$. Since BFGS stores V_k at each iteration, it requires sufficient computer memory.

2.3.3. The Nelder–Mead algorithm

NM is a gradient-free, unconstrained nonlinear optimization algorithm that was proposed in 1965 by Nelder and Mead [34]. NM uses a simplex to find an optimal solution for the n -dimensional optimization problems. NM starts with a set of $n + 1$ points which are the vertices of working simplex. Once the initial simplex is constructed, the objective function is evaluated at each vertices to test if the convergence criterion is satisfied, if not, NM transforms the simplex by using reflection, expansion, contraction, and shrinking operators. NM can be easily implemented and gives significant results in the first few iterations; however, it is not efficient for the large problems for which it does not guarantee an optimal solution.

2.3.4. The simulated annealing algorithm

Annealing is the process of changing the internal structure of the metals by heating them up to the melting point and slowly cooling into a minimum energy crystalline structure. SA is a gradient-free, heuristic search algorithm that was inspired by the annealing process in metal works and adapted to optimization problems by Kirkpatrick et al. [35]. The algorithm does not only accept the solutions that decrease the objective function, but also accepts the solutions that increase the objective function with a probability $p = e^{-\Delta/t}$ in order to avoid getting stuck in local minima, where Δ is the increase in the objective function and t is the control parameter. Probability of accepting bad solutions systematically decreases with the iterations. Similar to NM, SA tends to be slow for large problems and does not guarantee an optimal solution.

In the following section, the performances of the wind speed distributions and optimization algorithms are evaluated via model assessment criteria.

2.4. Model assessment

Wind speed distributions used in this study were evaluated based on K-S test, RMSE, R^2 , and PDE criteria. K-S test was used for deciding whether a sample belongs to a population with a specific distribution. Let $F_0(x)$ be the population cumulative distribution and $S_N(x)$ be the observed cumulative step function of sample, then test statistic d is the maximum difference between the empirical and analytical cumulative distributions [36].

$$d = \max |F_0(x) - S_N(x)|. \tag{30}$$

RMSE indicates the deviation between the observed data points and model’s predicted values. R^2 shows how well the model fits the observed data. RMSE and R^2 are respectively given below:

$$RMSE = \left[\frac{\sum_{i=1}^n \left(\hat{F}(X_{(i)}) - \frac{i}{n+1} \right)^2}{n} \right]^{1/2} \tag{31}$$

and

$$R^2 = 1 - \frac{\sum_{i=1}^n \left(\hat{F}(X_{(i)}) - \frac{i}{n+1} \right)^2}{\sum_{i=1}^n \left(\hat{F}(X_i) - \bar{\hat{F}}(X_i) \right)^2}, \tag{32}$$

where \hat{F} is the estimated *cdf*, $X_{(i)}$ is the i -th order statistics, $\bar{\hat{F}} = \sum_{i=1}^n \hat{F}_i/n$, and n is the number of wind speed observations [18]. PDE is described as follows:

$$PDE = \left| \frac{P_R - P_D}{P_R} \right| \times 100, \tag{33}$$

where P_R is the wind power density computed from the actual wind speed observations. P_D is the wind power density obtained from a theoretical density function. P_R and P_D are respectively given by:

$$P_R = \frac{1}{2} \rho \frac{1}{n} \sum_{i=1}^n v_i^3 \tag{34}$$

and

$$P_D = \frac{1}{2} \rho \int_0^\infty v^3 f_D(v) dv. \tag{35}$$

Lower K-S test statistic, RMSE and PDE values, and higher R^2 value indicate better fit performance.

3. Results

3.1. Seasonal wind speed analysis

The seasonal wind speed observations were gauged at 80 m height and collected on 10-min basis in Belen Wind Power Plant located in Hatay region of Turkey. Geographical coordinates of the plant is 36°28'42.2''N, 36°12'45.0''E. A preprocessing stage was not employed to the dataset. Table 1 shows the summary of wind speed for each season and year. Accordingly, summer months are more convenient for wind power generation.

Table 1. Descriptive statistics of the wind speed data (m/s) obtained from Belen Wind Power Plant.

Period	2013				2014			
	Mean	Std. Dev.	Min	Max	Mean	Std. Dev.	Min	Max
Winter	6.83	3.75	0.40	24.90	6.58	3.44	0.40	22.20
Spring	6.89	3.18	0.40	22.50	7.48	3.01	0.40	24.40
Summer	9.20	2.28	0.60	18.40	9.79	2.42	0.70	19.10
Autumn	5.89	2.91	0.40	21.90	5.85	2.88	0.40	21.00
Annual	7.29	3.33	0.40	24.90	7.38	3.26	0.40	24.40

Figure 3 presents the frequency of wind directions and the average wind speed for each direction and calm (wind speed <2 m/s). Maximum occurrence is at NNW with the average wind speed of 7.83 m/s.

The parameter estimations, K-S test statistic, RMSE, R^2 values, and the computation times of the wind speed distributions obtained by using four different optimization algorithms are presented in Tables 2 and 3. According to the results of K-S test statistic, WW was the most successful distribution in 2013. WW provided the best fit in winter and spring by using BFGS, and in autumn by using NM. NN was the second-best distribution and provided the best fit in summer by using NR. When the results were evaluated according to the RMSE and R^2 criteria, WW provided the best fit in winter by using NR and in spring by using BFGS. NN and LL provided the best fit by using NR in summer and autumn, respectively. According to the evaluation based on PDE, LL using NM and SA provided better modeling in winter and autumn, respectively.

In 2014, GG provided the best fit in all months according to K-S test statistic, RMSE, and R^2 criteria. For the K-S test statistic, GG provided better modeling by using NM in winter and spring, and NR in summer

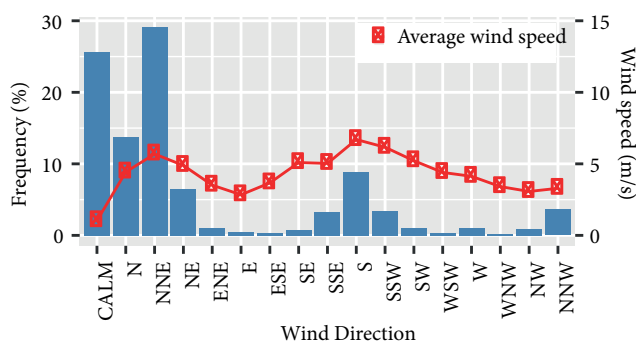


Figure 3. Wind direction frequency distributions of Belen Wind Power Plant.

and autumn. According to RMSE and R^2 criteria, GG provided the best fit by using BFGS in winter, NM in spring and summer, and NR in autumn. LL provided the best fit in winter and autumn by using NM according to the PDE criterion. Density fit plots are demonstrated in Figure 4.

In summary, mixture wind speed distributions outperformed the unimodal wind speed distributions according to K-S test statistic, RMSE, and R^2 criteria. Unimodal distributions performed better only in 3 seasons according to the PDE criterion. NM and BFGS were the fastest optimization algorithms for the parameter estimations of unimodal and mixture distributions, respectively. SA was the slowest algorithm for all types of distributions. Overall comparison of the distributions and the optimization algorithms is presented in Table 4.

Table 4. Overall comparison of the distributions and the optimization methods for the dataset obtained from Belen Wind Farm.

Date		KS		RMSE		R^2		PDE	
Year	Season	Model	Method	Model	Method	Model	Method	Model	Method
2013	Winter	WW	BFGS	WW	NR	WW	NR	LL	NM
	Spring	WW	BFGS	WW	BFGS	WW	BFGS	Gamma	SA
	Summer	NN	NR	NN	NR	NN	NR	Lognormal	SA
	Autumn	WW	NM	LL	NR	LL	NR	LL	SA
2014	Winter	GG	NM	GG	BFGS	GG	BFGS	LL	NM
	Spring	GG	NM	GG	NM	GG	NM	NN	NR
	Summer	GG	NR	GG	NM	GG	NM	Lognormal	BFGS
	Autumn	GG	NR	GG	NR	GG	NR	LL	NM

3.2. Annual wind speed analysis

Wind speed dataset observed at Gökçeada Meteorological Station was used for the annual wind speed analysis. Observations were gauged at 10 m height on hourly basis from 2010 to 2013. Geographical coordinates of the station is 40°11'27.6"N, 25°54'27.0"E. The dataset was provided by the Turkish State Meteorological Service. Table 5 presents the summary statistics for the dataset.

Wind direction frequency and the average wind speed for each direction and calm are presented in Figure 5. The maximum frequency of occurrence is at NNE with the average wind speed of 5.69 m/s.

The parameter estimations, K-S test statistic, RMSE, R^2 values, and the computation times of the wind speed distributions obtained by using four different optimization methods are presented in Table 6.

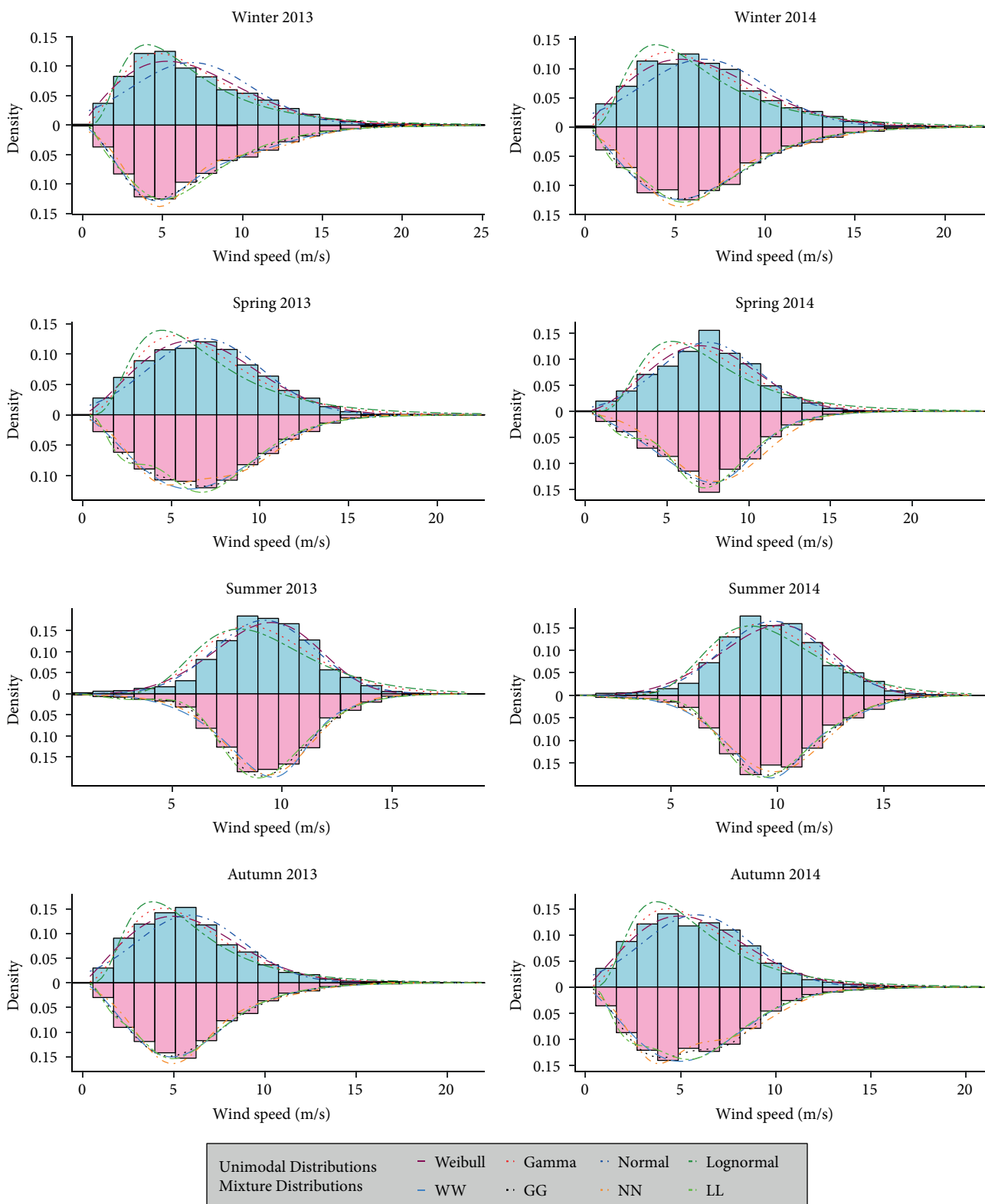


Figure 4. Unimodal and mixture density fits for the dataset obtained from Belen Wind Power Plant. The upper sides of the mirrored histograms present the unimodal density fits where the opposite sides present the mixture density fits.

Table 5. Descriptive statistics of the wind speed data (m/s) of Gökçeada Meteorological Station.

	Years			
	2010	2011	2012	2013
Mean	4.40	4.50	4.18	3.69
Std. Dev.	3.08	2.74	2.64	2.47
Min	0.10	0.10	0.20	0.10
Max	16.90	16.90	14.90	16.90

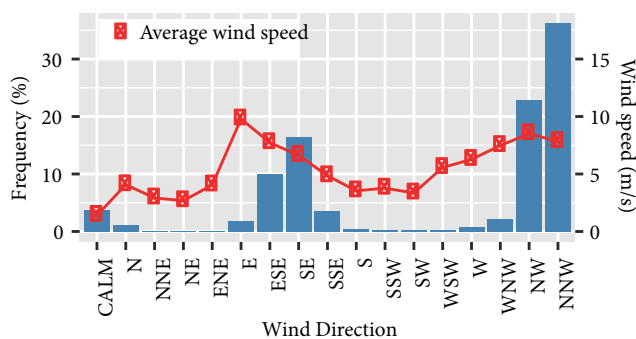


Figure 5. Wind direction frequency distributions of Gökçeada Meteorological Station.

GG is the most successful distribution which provides the best fit in 2010, 2011, and 2013 according to the K-S test statistic, RMSE, and R^2 criteria. According to the K-S test statistic, GG provided better modeling by using NM in 2010, SA in 2011, and BFGS in 2013. For the RMSE and R^2 criteria, GG provided the most efficiency by using SA in 2010 and NR in 2011 and 2013. WW by using NM was the second-best distribution and provided the best fit in 2012 according to the K-S test statistic, RMSE, and R^2 criteria. LL was the most successful distribution based on the PDE criterion, it used NM in 2010 and 2012, SA in 2011, and NR in 2013.

NM was the fastest optimization algorithm for unimodal wind speed distributions while BFGS and NM were the fastest algorithms for mixture distributions. SA is the slowest algorithm for all types of datasets. Density fit plots of the distributions are presented in Figure 6. Overall comparison of the distributions and optimization algorithms is presented in Table 7.

4. Discussion

In this paper, we presented a comparison between unimodal and two-component mixture wind speed distributions. The Weibull, gamma, normal, lognormal distributions, and their two-component mixture forms were employed to model the wind speed observations obtained from Belen Wind Power Plant and Gökçeada Meteorological Station.

Similar studies have been conducted in wind speed modeling; however, the aspects that make this study different are that it has a detailed seasonal and annual analysis and gives opportunity to compare the optimization algorithms for ML. Additionally, it also allows to compare the results of the wind speed datasets obtained from an actual wind farm and a random meteorological station. Finally, we would like to emphasize that the number of mixture components is fixed. In future works, we will focus on an unknown number of mixture components for wind speed modeling.

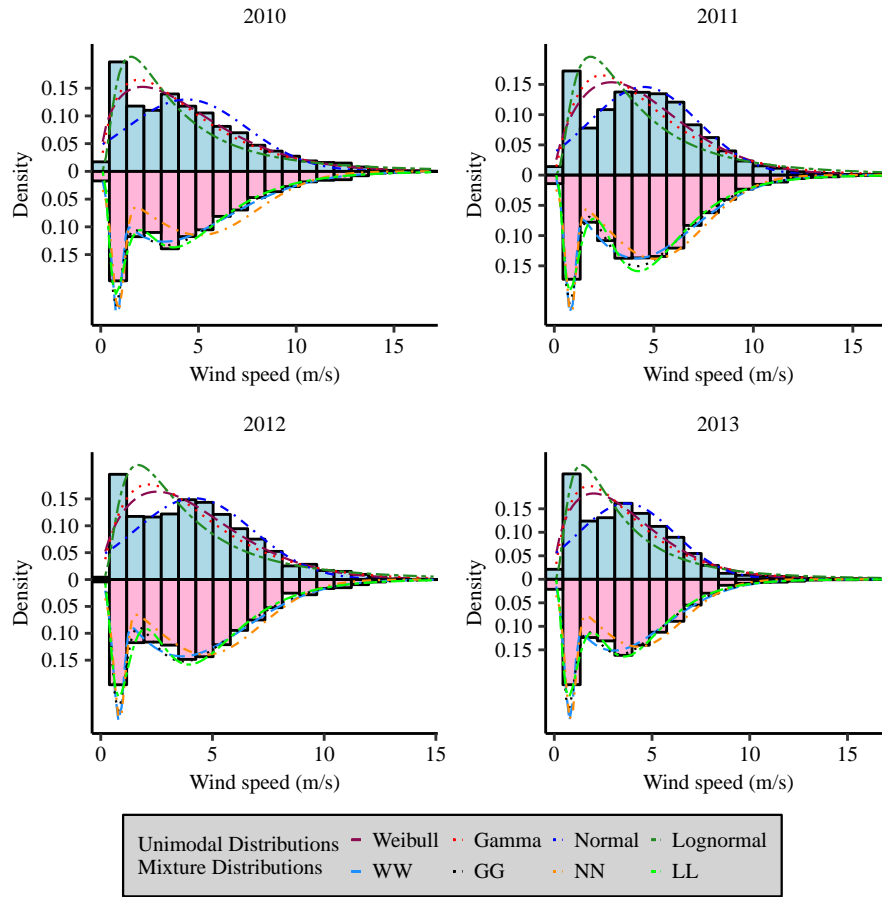


Figure 6. Unimodal and mixture density fits for the dataset obtained from Gökçeada Meteorological Station. The upper sides of the mirrored histograms present the unimodal density fits where the opposite sides present the mixture density fits.

Table 7. Overall comparison of the distributions and optimization methods for the dataset obtained from Gökçeada Meteorological Station.

Date	KS		RMSE		R^2		PDE	
	Model	Method	Model	Method	Model	Method	Model	Method
2010	GG	NM	GG	SA	GG	SA	LL	NM
2011	GG	SA	GG	NR	GG	NR	LL	SA
2012	WW	NM	WW	NM	WW	NM	LL	NM
2013	GG	BFGS	GG	NR	GG	NR	LL	NR

5. Conclusion

Main results of this study can be summarized as follows:

1. Two-component mixture distributions have superiority over the unimodal distributions for the seasonal and annual wind speed data according to the assessment criteria including K-S test statistic, RMSE, R^2 , and PDE.

2. For the dataset obtained from Belen Wind Power Plant, WW performed better than other distributions in 2013 and GG performed better than others in 2014.
3. GG was the most efficient distribution for the dataset obtained from Gökçeada Meteorological Station.
4. Best model chosen for each time period shows more variability for the dataset obtained from Belen Wind Power Plant; therefore, single distribution may not be sufficient for modeling the wind speed data observed at wind farms.
5. NM is the fastest algorithm in parameter estimation of unimodal wind speed distributions.
6. BFGS and NM are the fastest algorithms in parameter estimation for the mixture wind speed distributions.
7. SA is the slowest algorithm for all datasets.

Acknowledgments

The authors thank the anonymous referees for valuable comments and insightful suggestions. This study is based on an ongoing doctoral thesis by the first author. This work was supported by the Scientific Research Projects Coordination Unit of Mehmet Akif Ersoy University. Project number 0440-DR-17.

References

- [1] Çelik, AN. A techno-economic analysis of wind energy in Southern Turkey. *Int J Green Energy* 2007; 4 (3): 233-247. doi: 10.1080/15435070701338358
- [2] Akpınar S, Akpınar EK. Estimation of wind energy potential using finite mixture distribution models. *Energ Convers Manage* 2009; 50 (4): 877-884. doi: 10.1016/j.enconman.2009.01.007
- [3] Kaygusuz K. Renewable and sustainable energy use in Turkey: a review. *Renew Sust Energ Rev* 2002; 6 (4): 339-366. doi: 10.1016/S1364-0321(01)00007-7
- [4] Arslan T, Bulut YM, Yavuz AA. Comparative study of numerical methods for determining Weibull parameters for wind energy potential. *Renew Sust Energ Rev* 2014; 40: 820-825. doi: 10.1016/j.rser.2014.08.009
- [5] IEA (International Energy Agency). *Renewables Information 2016*, Paris, France: IEA, 2016. doi: 10.1787/renew-2016-en
- [6] Safari B. Modeling wind speed and wind power distributions in Rwanda. *Renew Sust Energ Rev* 2011; 15 (2): 925-935. doi: 10.1016/j.rser.2010.11.001
- [7] Hou Y, Peng Y, Johnson AL, Shi J. Empirical analysis of wind power potential at multiple heights for North Dakota wind observation sites. *Energ Sci Tech* 2012; 4 (1): 1-9. doi: 10.3968/j.est.1923847920120401.289
- [8] Sohoni V, Gupta S, Nema R. A comparative analysis of wind speed probability distributions for wind power assessment of four sites. *Turk J Elec Eng & Comp Sci* 2016; 24 (6): 4724-4735. doi: 10.3906/elk-1412-207
- [9] Kaplan YA. The evaluating of wind energy potential of Osmaniye region with using Weibull and Rayleigh distributions. *SDU J Nat Appl Sci* 2016; 20 (1): 62-71 (in Turkish with an abstract in English). doi: 10.19113/sdufbed.63806
- [10] Köse R, Özgür MA, Erbaş O, Tuğcu A. The analysis of wind data and wind energy potential in Kütahya, Turkey. *Renew Sust Energ Rev* 2004; 8 (3): 277-288. doi: 10.1016/j.rser.2003.11.003
- [11] Çelik AN. A statistical analysis of wind power density based on the Weibull and Rayleigh models at the southern region of Turkey. *Renew Energ* 2003; 29 (4): 593-604. doi: 10.1016/j.renene.2003.07.002
- [12] Akpınar EK, Akpınar S. Determination of the wind energy potential for Maden-Elazığ, Turkey. *Energ Convers Manage* 2004; 45 (18-19): 2901-2914. doi: 10.1016/j.enconman.2003.12.016

- [13] Gökçek M, Bayülken A, Bekdemir Ş. Investigation of wind characteristics and wind energy potential in Kırklareli, Turkey. *Renew Energ* 2007; 32 (10): 1739-1752. doi: 10.1016/j.renene.2006.11.017
- [14] Akgül FG, Şenoğlu B, Arslan T. An alternative distribution to Weibull for modeling wind speed data: Inverse Weibull distribution. *Energ Convers Management* 2016; 114: 234-240. doi: 10.1016/j.enconman.2016.02.026
- [15] Kantar YM, Usta İ. Analysis of wind speed distributions: wind distribution function derived from minimum cross entropy principles as better alternative to Weibull function. *Energ Convers Manage* 2008; 49 (5): 962-973. doi: 10.1016/j.enconman.2007.10.008
- [16] Kantar YM, Usta İ. Analysis of the upper-truncated Weibull distribution for wind speed. *Energ Convers Manage* 2015; 96: 81-88. doi: 10.1016/j.enconman.2015.02.063
- [17] Mert İ, Karakuş C. A statistical analysis of wind speed data using Burr, generalized gamma, and Weibull distributions in Antakya, Turkey. *Turk J Elec Eng & Comp Sci* 2014; 23 (6): 1571-1586. doi: 10.3906/elk-1402-66
- [18] Arslan T, Acıtaş Ş, Şenoğlu B. Generalized Lindley and power Lindley distributions for modeling the wind speed data. *Energ Convers Manage* 2017; 152: 300-311. doi: 10.1016/j.enconman.2017.08.017
- [19] Kantar YM, Usta İ, Arık İ, Yenilmez İ. Wind speed analysis using the extended generalized Lindley distribution. *Renew Energ* 2018; 118: 1024-1030. doi: 10.1016/j.renene.2017.09.053
- [20] Morgan EC, Lackner M, Vogel RM, Baise LG. Probability distributions for offshore wind speeds. *Energ Convers Manage* 2011; 52 (1): 15-26. doi: 10.1016/j.enconman.2010.06.015
- [21] Kollu R, Rayapudi SR, Narasimham SVL, Pakkurthi KM. Mixture probability distribution functions to model wind speed distributions. *Int J of Energy Environ Eng* 2012; 3 (1): 27. doi: 10.1186/2251-6832-3-27
- [22] Carta JA, Ramirez P. Use of finite mixture distribution models in the analysis of wind energy in the Canarian Archipelago. *Energ Converse Manage* 2007; 48 (1): 281-291. doi: 10.1016/j.enconman.2006.04.004
- [23] Usta İ, Kantar YM. Analysis of some flexible families of distributions for estimation of wind speed distributions. *Appl Energ* 2012; 89 (1): 355-367. doi: 10.1016/j.apenergy.2011.07.045
- [24] Chang, TP. Estimation of wind energy potential using different probability density functions. *Appl Energ* 2011; 88 (5): 1848-1856. doi: 10.1016/j.apenergy.2010.11.010
- [25] Akdağ SA, Bagiorgas HS, Mihalakakou G. Use of two-component Weibull mixtures in the analysis of wind speed in the Eastern Mediterranean. *Appl Energ* 2010; 87 (8): 2566-2573. doi: 10.1016/j.apenergy.2010.02.033
- [26] Jaramillo OA, Borja MA. Wind speed analysis in La Ventosa, Mexico: a bimodal probability distribution case. *Renew Energ* 2004; 29 (10): 1613-1630. doi: 10.1016/j.renene.2004.02.001
- [27] Shin JY, Ouarda TBMJ, Lee T. Heterogeneous mixture distributions for modeling wind speed, application to the UAE. *Renew Energ* 2016; 91: 40-52. doi: 10.1016/j.renene.2016.01.041
- [28] Mazzeo D, Oliveti G, Labonia E. Estimation of wind speed probability density function using a mixture of two truncated normal distributions. *Renew Energ* 2018; 115: 1260-1280. doi: 10.1016/j.renene.2017.09.043
- [29] Henningsen A, Toomet O. maxLik: A package for maximum likelihood estimation in R. *Computation Stat* 2010; 26 (3): 443-458. doi: 10.1007/s00180-010-0217-1
- [30] Broyden CG. The convergence of a class of double-rank minimization algorithms 1. general considerations. *J Inst Math Appl* 1970; 6 (1): 76-90. doi: 10.1093/imamat/6.1.76
- [31] Fletcher R. A new approach to variable metric algorithms. *Comput J* 1970; 13 (3): 317-322. doi: 10.1093/comjnl/13.3.317
- [32] Goldfarb D. A family of variable metric updates derived by variational means. *Math Comput* 1970; 24 (109): 23-26. doi: 10.2307/2004873

- [33] Shanno DF. Conditioning of quasi-newton methods for function minimization. *Math Comput* 1970; 24 (111): 647-656. doi: 10.2307/2004840
- [34] Nelder JA, Mead R. A simplex algorithm for function minimization. *Comput J* 1965; 7 (4): 308-313. doi: 10.1093/comjnl/7.4.308
- [35] Kirkpatrick S, Gelatt Jr CD, Vecchi PM. Optimization by simulated annealing. *Science* 1983; 220 (4598): 671-680. doi: 10.1126/science.220.4598.671
- [36] Massey Jr FJ. The Kolmogorov-Smirnov Test for Goodness of Fit. *J Am Stat Assoc* 1951; 46 (253): 68-78. doi:10.1080/01621459.1951.10500769